ISSN 1807-1929
Revista Brasileira de Engenharia Agrícola e Ambiental
Brazilian Journal of Agricultural and Environmental Engineering
v.30, n.9, e303956, 2026
Campina Grande, PB – http://www.agriambi.com.br – http://www.scielo.br/rbeaa

DOI: https://doi.org/10.1590/1807-1929/agriambi.v30n9e303956 ORIGINAL ARTICLE

# Irrigation management alters energy partitioning, crop coefficients, and productivity of 'Tahiti' acid lime[1]

## Manejo da irrigação altera partição energética, coeficientes de cultivo e produtividade da limeira ácida 'Tahiti'

Tayssa M. Franco[2*], Matheus L. Rua[2], Miguel G. M. Santos[2], Paulo A. S. Pardim[2], Jheny T. de S. Favacho[2], Jadson de J. R. de Pinho[2], Marcus J. A. de Lima[2], Vandeilson B. Moura[2] & Paulo J. de O. P. de Souza[2]

[1] Research developed at Lima Citrus Farm, Capitão Poço, Pará, Brazil
[2] Universidade Federal Rural da Amazônia, Belém, Pará, Brazil

*HIGHLIGHTS:*

*Irrigation alters energy partitioning in the system, leading to increased sensible heat dissipation during dry periods.*
*Differences in crop coefficients reflect water limitations and variations in evapotranspiration under atmospheric demand.*
*The irrigated system promoted significant yield gains in both 'Tahiti' acid lime off-seasons.*

**ABSTRACT:** Climate variability poses a major challenge to tropical citrus production, especially in regions with marked water seasonality. This study aimed to evaluate the effects of irrigated and rainfed regimes on the crop coefficient, energy partitioning, and yield of 'Tahiti' acid lime grafted onto Swingle citrumelo. The study was conducted from 2023 to 2025 in Capitão Poço, Pará State, Brazil, using a completely randomized design with two treatments (irrigated and rainfed) and 10 replications, totaling 20 plots. Micrometeorological data were obtained from an automatic weather station installed in the experimental area, and crop evapotranspiration (ETc) was estimated using the soil water balance method. An irrigation depth of 4.42 mm (66.3 L) per plant per day was sufficient to increase the average fruit yield and to concentrate 50.8% of the 2024 agricultural production during the off-season. During dry periods, the irrigated regime showed an average ETc of 3.7 mm per day and a crop coefficient (Kc) of 1.0, both indicating conditions close to atmospheric evaporative demand. In contrast, the rainfed regime had an average ETc of 2.9 mm per day and a Kc of 0.8. Despite the yield increase, radiation balance analysis revealed sensible heat flux values approaching latent heat flux values, indicating differences in flux partitioning under drip irrigation. Total yield was higher in the irrigated system (40.67 t ha$^{-1}$) compared to the rainfed system (19.50 t ha$^{-1}$), with significantly greater yields during the off-season.

**Key words:** *Citrus latifolia* Tanaka, evapotranspiration, rainfed cultivation, tropical fruit growing

**RESUMO:** A variabilidade climática representa um desafio à citricultura tropical, sobretudo em regiões com marcada sazonalidade hídrica. Objetivou-se avaliar os efeitos dos regimes irrigado e sequeiro sobre o coeficiente de cultivo, a partição de energia e a produtividade da limeira ácida 'Tahiti' enxertada em Citrumelo Swingle. O estudo foi conduzido entre os anos de 2023 e 2025, em Capitão Poço, PA, Brasil, em delineamento inteiramente casualizado, com dois tratamentos (irrigado e sequeiro) e 10 repetições totalizando 20 parcelas. Dados micrometeorológicos foram obtidos por uma estação automática instalada na área experimental, a evapotranspiração da cultura (ETc) foi estimada pelo balanço hídrico do solo. A lâmina de irrigação de 4,42 mm (66.3 L) por planta por dia aumentou a produtividade média de frutos e concentrou 50,8% da produção agrícola de 2024 no período de entressafra. Nos meses menos chuvosos, a ETc média das plantas irrigadas foi de 3,7 mm por dia com coeficiente de cultura (Kc) de 1,0, valores próximos à demanda atmosférica, enquanto as plantas em sequeiro apresentaram ETc média de 2,9 mm por dia e Kc de 0,8. Apesar do incremento produtivo, observou-se partição do saldo de radiação com fluxos de calor sensível próximos ao calor latente, indicando diferenças na partição do fluxo sob irrigação por gotejamento. A produtividade total foi superior no sistema irrigado (40,67 t ha$^{-1}$) em relação ao sequeiro (19,50 t ha$^{-1}$), com rendimentos significativamente maiores nas entressafras.

**Palavras-chave:** *Citrus latifolia* Tanaka, evapotranspiração, cultivo de sequeiro, fruticultura tropical

Ref. 303956 – Received 19/01/2026
* Corresponding author - E-mail: tayssa.menezes2015@gmail.com
• Accepted 11/05/2026 • Published 27/08/2026
Editors: Edivan Rodrigues de Souza & Hans Raj Gheyi

**Publisher's Note:** The statements, opinions, and data contained in this article are the sole responsibility of the author(s). The Agriambi Journal and/or Editor(s) disclaim any liability for damages to persons or property resulting from any ideas, methods, instructions, or products mentioned in the article.

This is an open-access article distributed under the Creative Commons Attribution 4.0 International License.

## Introduction

The 'Tahiti' acid lime (*Citrus latifolia* Tanaka) is a hybrid fruit crop resulting from the cross between the Sicilian lemon and the Persian lime. The commercialization of its fruits spans several sectors, from fresh fruit consumption in domestic and international markets to their use by the juice, pharmaceutical, and cosmetic industries (Diana et al., 2021).

In 2024, Brazil produced more than 1.72 million tons of Tahiti lime, with the Southeast region accounting for over 81% of this total. The North region ranked third in that year, with 97 thousand tons (5.6%), and within this region, the state of Pará stood out with a production of 74.44 thousand tons of this fruit (IBGE, 2025).

This scenario has driven the emergence of new citrus production hubs, such as that in northeastern Pará, where the municipality of Capitão Poço is prominent (Silva Júnior et al., 2023). However, as previously mentioned, the production volume in the Southeast surpasses that of other Brazilian regions, not only in planted area but also in productivity (30 t $ha^{-1}$). This clearly highlights the need for further studies and technological adjustments to enhance productivity in the Amazonian environment.

Citrus production in Pará is located within the equatorial belt and presents edaphoclimatic characteristics typical of Eastern Amazonia, which differentiate it from other producing regions in the country (Silva Júnior et al., 2023). Rainfall distribution is irregular, and its volume decreases significantly during the second half of the year. This period is also marked by high temperatures and low air humidity (Pinto et al., 2022). As a result, many crops are subject to water deficit and canopy overheating due to greater heat dissipation through sensible heat flux (Bagley et al., 2017), making the use of irrigation technologies indispensable to ensure high yields.

Crop productivity is strongly associated with photosynthetic efficiency and carbon assimilation. Soils with moisture levels close to field capacity favor transpiratory fluxes, making transpiration a physical process mainly dependent on vapor pressure deficit. As the soil dries, biological factors influence the process, as the plant interacts with the environment by reducing stomatal opening and, consequently, its conductance (Oliveira et al., 2024). In this context, understanding local energy dynamics, crop water demand, and the reproductive cycle becomes essential.

In this context, it is hypothesized that irrigation management during the dry period significantly alters energy partitioning, crop coefficients, and the productivity of ‚Tahiti' acid lime. Thus, this study aimed to evaluate the effects of irrigated and rainfed regimes on energy partitioning, crop evapotranspiration (ETc), crop coefficients (Kc), and the productivity of 'Tahiti' acid lime grafted onto Swingle citrumelo in northeastern Pará.

## Material and Methods

The experiment was conducted between July 2023 and January 2025 in a commercial orchard at Lima Cítros Farm, located in the municipality of Capitão Poço, in the northeastern mesoregion of the state of Pará, Brazil (01° 47′ 28″ S; 47° 05′ 51″ W). The experimental area comprised six plots, totaling 100 ha. A micrometeorological monitoring tower was installed at the end of the first plot, and the northeast direction presented the highest wind frequency and intensity and frequency during the experimental period.

The region has a humid tropical climate, subtype Ami, according to the Köppen classification (Alvares et al., 2013). The mean annual total precipitation is approximately 2,401 mm, with the months from September to November presenting the lowest rainfall indices (7.1% of the annual rainfall). Air temperature ranges from 21.4 to 32.7 °C, with a mean relative humidity of 83%, which may decrease to around 75% in November (Pacheco & Bastos, 2001).

The orchard consisted of 12-year-old 'Tahiti' acid lime plants grafted onto Swingle citrumelo (× *Citroncirus* spp.). Each plant occupied an area of 15 $m^2$, arranged in a spacing of 5 m between rows and 3 m between plants, resulting in a density of 666.67 plants $ha^{-1}$.

The soil was classified as Oxisol with a sandy clay loam texture (Soil Survey Staff, 2022). The chemical characteristics were determined for the 0–20 and 20–40 cm soil layers where as the physical and hydraulic properties were determined for the 0–40 cm soil layer. The results are presented in Table 1.

**Table 1.** Chemical characteristics of the soil at 0–20 and 20–40 cm and physical and hydraulic properties of the 0–40 cm soil layer in an area cultivated with 'Tahiti' acid lime

| Layer (cm) | Chemical characteristics | | | | | | | | | | | | |
|---|---|---|---|---|---|---|---|---|---|---|---|---|---|
| | N | P | K | Na | Al | Ca | Ca + Mg | pH $H_2O$ | H + Al | CEC | | Saturation | |
| | | | | | | | | | | Total | Effective | Bases | Aluminum |
| | % | ------- mg $dm^{-3}$ ------- | | | ----- $cmol_c$ $dm^{-3}$ ----- | | | | $cmol_c$ $dm^{-3}$ | --- $cmol_c$ $dm^{-3}$ --- | | % | % |
| 0-20 | 0.08 | 6.3 | 230.8 | 2.63 | 0 | 3.46 | 3.79 | 5.63 | 1.84 | 6.23 | 4.39 | 70.51 | 0 |
| 20-40 | 0.05 | 0.72 | 181.88 | 0.75 | 0.04 | 1.1 | 1.95 | 5.65 | 1.28 | 3.69 | 2.46 | 65.49 | 1.63 |

| Layer (cm) | ---------- Physical characteristics ---------- | | | | | ---------- Soil moisture ---------- | | |
|---|---|---|---|---|---|---|---|---|
| | Fine sand | Coarse sand | Silt | Clay | BD | FC | PWP | Critical |
| | ---------- g $kg^{-1}$ ---------- | | | | kg $dm^{-3}$ | ---------- $cm^3$ $cm^{-3}$ ---------- | | |
| 0-40 | 402.2 | 282.0 | 102.5 | 213.3 | 1.58 | 0.20 | 0.11 | 0.12 |

CEC - Cation Exchange Capacity, BD - Soil bulk density; FC - Field capacity; PWP - Permanent wilting point

Localized irrigation was applied using a drip tape system. Irrigation was carried out from September to November 2023 and from August to November 2024.

Irrigation management was performed daily, and a fixed irrigation depth was used due to the farm's routine and labor availability. A mean reference evapotranspiration of 5 mm per day (Allen et al., 1998), adjusted by a crop coefficient of 0.84, was considered. This value corresponds to the maximum coefficient recorded for 'Tahiti' acid lime aged between 6 and 7 years in the same municipality (Pinto et al., 2022). An irrigation system efficiency (E) of 95% was assumed to correct the applied depth. Each plant was equipped with six emitters at a flow rate of 2.5 L $h^{-1}$, and the system operated for 4 hours and 25 min, totaling 66.3 L per plant per day, corresponding to an irrigation depth of 4.42 mm per plant. The wetted strip formed by the irrigation system was 1 m wide. The irrigation depth was calculated based on Eq. 1.

$$L = \frac{(ETo \times Kc)}{E} \quad (1)$$

Where:

L – irrigation depth (mm per day);

ETo – reference evapotranspiration, considering a mean value of 5 mm per day;

Kc – crop coefficient, with a value of 0.84; and,

E – irrigation system efficiency (0.95).

The crop coefficient (Kc) was determined as the ratio of crop evapotranspiration (ETc) to reference evapotranspiration (ETo), and was correlated with crop development stage and climatic conditions of the study area (Schwenck et al., 2020). Reference evapotranspiration (ETo) was estimated using the Penman–Monteith method (FAO 56) (Allen et al., 1998).

Agronomic monitoring of the experiment was conducted in a completely randomized design with two treatments (irrigated and rainfed) and ten replications, totaling 20 experimental units. The experimental units were randomized within planting rows near the monitoring tower; in one row, plants were managed under the irrigated regime, while in the adjacent row, plants were managed under the rainfed regime.

For the analysis of production variation (t $ha^{-1}$) throughout the experiment and yield (kg per plant) during the off-season periods, all fruits with diameters greater than 4 cm were harvested. A total of ten harvests were performed, comprising two off-season periods from October to December in 2023 and 2024. The main harvest season occurred in February, April, June, and July 2024.

To obtain meteorological data, a microclimatic agrometeorological monitoring tower was installed between the planting rows corresponding to the irrigated and rainfed treatments. Figure 1 shows the schematic layout of the field instrumentation and sensor arrangement. Sensors were connected to a datalogger, with readings taken every 10 s and averages recorded every 10 min.

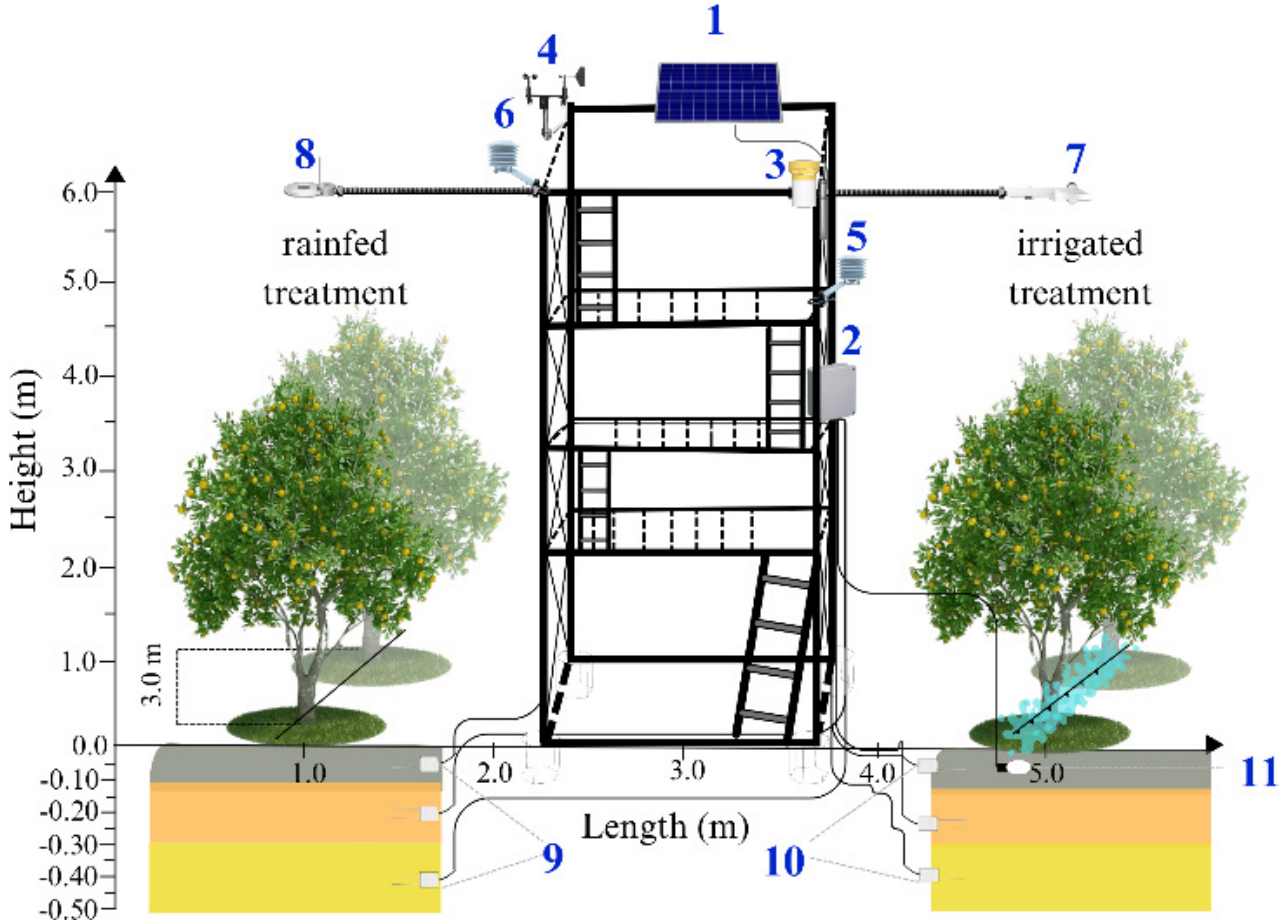


1 – Solar panel; 2 – Shelter with datalogger (CR100, Campbell Scientific, Inc., Logan, UT, USA); 3 – Rain gauge (TB4, Campbell Scientific Instrument, Logan, UT, USA); 4 – Cup anemometer (03002, RM Young, Traverse City, MI, USA); 5 – Thermohygrometers (MX2301A, HOBO); 6 – Thermohygrometer (HMP155A, Campbell Scientific Instrument, Logan, UT, USA); 7 – Four-component net radiometer (CNR4, Campbell Scientific); 8 – Net radiometer (NR-Lite, Campbell Scientific, Logan, UT, USA); 9 and 10 – Soil water content reflectometers (CS616, Campbell Scientific Instrument, Logan, UT, USA at –0.10 m; and CS615, Campbell Scientific Instrument, Logan, UT, USA at –0.30 and –0.50 m); 11 – soil heat flux plate (Hukseflux, HFP01)

**Figure 1.** Schematic representation of the monitoring tower instrumentation and its position relative to the planting rows

Sensors 3, 4, and 6 were used to measure monthly precipitation, wind speed and direction, air temperature and relative humidity, respectively. Periods with total monthly rainfall below 100 mm were considered dry periods (Marengo et al., 2011).

Soil volumetric water content was monitored using TDR-type sensors installed at depths of 0.10, 0.30, and 0.50 m (indices 9 and 10), as shown in Figure 1. To determine soil water storage (h), the trapezoidal rule was applied (Libardi, 2005) using Eqs. 2 and 3.

$$h_L = \int_0^1 \theta(Z)dZ \cong \left[0.5 \times \theta(Z_0) + \sum_{i=1}^{n-1} \theta(Z_i) + 0.5 \times \theta(Z_n)\right] * \Delta Z \quad (2)$$

Where:

$h_L$ – soil water storage for a given depth (mm);

$\theta$ (Z) – volumetric soil water content of each layer; and,

$\Delta Z$ –thickness of the soil layers.

$$\Delta h = h\ (final) - h(initial) \quad (3)$$

Where:

$\Delta h$ - variation in soil water storage (mm); and,

h - soil water storage (mm).

To determine saturated soil hydraulic conductivity (Ks), double-ring infiltrometer tests were carried out near the plants where TDR sensors were installed in both treatments (Brandão et al., 2006). The resulting values were applied to the equation proposed by Soto & Kiang (2017) (Eq. 4). Drainage (D) and capillary rise (CR) in the monitored soil profile were estimated using the Darcy–Buckingham equation (Mualem, 1976; Eq. 5).

$$K_s = \left(Z_w \times \ln\left(\frac{H_1}{\frac{H_2}{t}}\right)\right) \quad (4)$$

Where:

$K_s$ – saturated soil hydraulic conductivity;

$Z_w$ – depth of the wetting front (cm);

$H_1$ and $H_2$ – are the water depths in the ring at the initial time (t0) and at time t, respectively; and,

t – time between the two readings.

$$q_z = -K(\theta) * \nabla\phi_t \quad (5)$$

Where:

$q_z$ – soil water flux density at depth z (mm per day);

$\nabla\phi_t$ – total potential gradient in the vertical soil direction (cm cm$^{-1}$); and,

K($\theta$) –unsaturated soil hydraulic conductivity (mm per day) (van Genuchten, 1980), with m = 1-1/n (Mualem, 1976).

To estimate the total vertical potential gradient ($\nabla\phi t$), tensiometers were installed near the monitored plants at depths of 20 and 40 cm. Tensiometer sensors were installed using a 20 mm screw-type auger. Tension readings were taken daily using a digital tensiometer. Matric potential was calculated according to Eq. 6.

$$\phi = (Z + h_1 - L) \times 0.0981 \quad (6)$$

Where:

$\Phi$ – matric potential (kPa);

Z – distance between the porous cup and the soil surface (m);

$h_1$ – height of water above the surface in the tensiometer (m); and,

L – tensiometer reading (m of water column).

To estimate actual crop evapotranspiration (ETc) for plants under irrigated and rainfed regimes, Eq. 7 was used.

$$ETc = \Delta h - P - I - D - CR \quad (7)$$

Where:

ETc – crop evapotranspiration (mm per day);

$\Delta h$ – variation in soil water storage (mm);

P – precipitation (mm);

I – irrigation depth (mm);

D – internal drainage (mm); and,

CR – capillary rise (mm).

The irrigated treatment was equipped with a four-component net radiometer, model CNR4 (index 7, Figure 1), which measured incoming shortwave radiation (S↓), reflected shortwave radiation (S↑), incoming longwave radiation (L↓), and reflected longwave radiation (L↑). Net radiation (Rn) for the irrigated treatment was calculated according to Eqs. 8, 9, and 10. Conversely, the NR-Lite net radiometer (index 8, Figure 1) installed in the rainfed treatment row directly measured Rn.

$$R_{ns} = S_\downarrow + S_\uparrow \quad (8)$$

$$R_{nl} = L_\downarrow + L_\uparrow \quad (9)$$

$$R_n = R_{ns} + R_{nl} \quad (10)$$

With Rn values obtained for both treatments, the surface energy balance for the irrigated surface was calculated according to Eq. 11.

$$Rn = H + G + LE \quad (11)$$

Where:

Rn – net radiation (MJ m$^{-2}$ per day);

H – sensible heat flux (MJ m$^{-2}$ per day);

G – soil heat flux (MJ m$^{-2}$ per day); and,

LE – latent heat flux (MJ m$^{-2}$ per day).

To determine LE for the treatments, the relationship between calculated ETc and the latent heat of vaporization of water ($\lambda$) was used, according to Eq. 12.

$$LE = ETc \times \lambda \quad (12)$$

Where:

LE – latent heat flux (MJ m$^{-2}$ per day);

ETc – crop evapotranspiration under the rainfed treatment (mm per day); and,

λ – latent heat of vaporization of water at 20–25 °C (assumed as 2.45 MJ $kg^{-1}$).

Soil heat flux (G) for the irrigated treatment was obtained using a heat flux plate sensor (Hukseflux, HFP01; index 11 in Figure 1). In contrast, soil heat flux for the rainfed treatment (Gest) was estimated using a multiple regression (adjusted $R^2$ = 0.89) relating G from the irrigated treatment to air temperature and relative humidity, as described in Eq. 13.

$$G_{est} = 110.52 - 18\ RH\ 3.36\ Tar \quad (13)$$

Where:

$G_{est}$ – estimated soil heat flux (MJ $m^{-2}$ per day);

RH – air relative humidity (%); and,

Tar – mean air temperature (°C).

To calculate sensible heat flux (H), values of net radiation (Rn), latent heat flux (LE), and soil heat flux (G) were used, according to Eq. 14

$$Rn = LE + H + G \quad (14)$$

$$H = Rn - LE - G$$

Surface albedo for the irrigated treatment was calculated as the ratio between reflected and incoming shortwave radiation (obtained from the CNR4 net radiometer), according to Eq. 15.

$$\alpha = \frac{S_{\uparrow}}{S_{\downarrow}}\ 100 \quad (15)$$

Where:

α – surface albedo (%);

$S_{\uparrow}$ – reflected shortwave radiation; and,

$S_{\downarrow}$ – incoming shortwave radiation.

All calculations and figures were produced using R software. For the statistical analysis of soil moisture values, differences between irrigated and rainfed conditions were evaluated using the Wilcoxon rank-sum test, since the data did not meet the assumption of normality ($p < 0.01$). For crop evapotranspiration (ETc) and the crop coefficient (Kc) under irrigated and rainfed conditions, differences between treatments were assessed using the paired t-test ($p < 0.01$). For production and productivity data during off-season periods, an independent-samples t-test was applied ($p < 0.01$). In all analyses involving the t-test, the assumptions of normality and homoscedasticity were verified.

## Results and Discussion

Figure 2 shows the monthly precipitation monitored in the 'Tahiti' acid lime orchard from July 2023 to January 2025. Overall, a well-defined and pronounced seasonality was observed. In 2023, the dry period (DP; precipitation < 100 mm per month) occurred from August to October, whereas in 2024 this period was longer, extending from July to November.

The total rainfall recorded during the dry period (DP) in 2023 was 113 mm, with a mean of 38 mm per month. In contrast, in 2024, the total rainfall during the DP was 94 mm, with a mean of 18.72 mm per month. A difference of approximately 49% was observed between the two years. Studies conducted with citrus crops emphasize that a marked reduction in precipitation during the dry months may indicate that plants are subjected to both water and thermal stress, due to higher air temperatures and a higher vapor pressure deficit (Silva et al., 2018; Pinto et al., 2022).

It is worth noting that the Amazon region was under the influence of a moderate-to-strong El Niño from May 2023 to April 2024 (NOAA, 2025). This phenomenon directly contributes to longer dry periods and reduced rainfall intensity during rainy seasons.

The persistence of El Niño conditions over consecutive years represents a large-scale climatic anomaly that has become increasingly frequent under the current climate change scenario (NOAA, 2025). Within this context, an increase in mean air temperature and a shortening of the rainy season are expected in some locations of Eastern Amazonia (Souza et al., 2016). Therefore, the use of technologies such as irrigation has become increasingly necessary to mitigate the impacts of potential water restrictions on crops.

On the other hand, in 2023, the months with rainfall exceeding 100 mm were July, November, and December, totaling 442 mm. In 2024, a total of 2,521 mm was recorded. March was the rainiest month in 2024, with an accumulated rainfall of 751 mm. This pattern is typical of regions with a humid tropical climate, where most of the annual precipitation

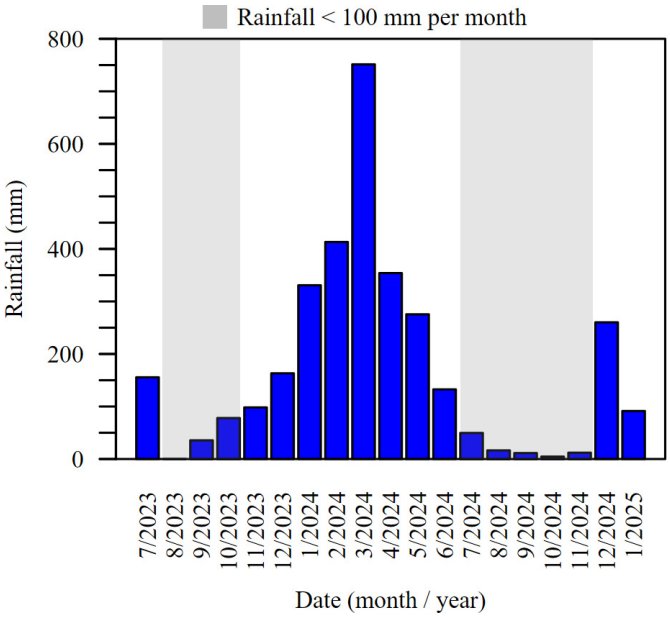


**Figure 2.** Monthly variation in rainfall (P, mm) from July 2023 to January 2025, with dry periods (P < 100 mm per month) identified from August to October 2023 and from July to November 2024

is concentrated in a few months, characterized by intense and short-duration rainfall events, generally associated with the Intertropical Convergence Zone (ITCZ) and tropical convective systems (Ribeiro et al., 2023).

Figure 3 presents the daily variability of mean, maximum, and minimum values of the meteorological elements relative humidity of air - RH (Figure 3A), air temperature - T (Figure 3B), and wind speed (Figure 3C).

Mean and minimum RH values during the rainy period (RP) were 80.6 and 60.5%, respectively. Mean RH values during the DP were 73.4% in 2023 and 73.1% in 2024. In contrast, mean minimum RH values were below 50% in both periods (49.5 and 48.1% in 2023 and 2024, respectively) (Figure 3A).

Previous studies on the climatology of the municipality addressed in the present study indicate that mean RH during the period from July to November has been decreasing, from 79.40% between 1980 and 1999 (Pacheco & Bastos, 2001) to 71.16% between 2011 and 2020 (Pinto et al., 2022). In the present study, the mean RH during the evaluation period was 77.4%, which is consistent with the historical variability reported for the region.

Figure 3B shows that, overall, mean maximum, mean, and minimum air temperatures during the RP were 31.9, 26.3, and 23.3 °C, respectively. The mean minimum temperature observed during the rainy period was 1.3 °C higher than that reported by Pacheco & Bastos (2001). However, mean maximum air temperatures during the dry periods of 2023 and 2024 were 32.8 and 34.04 °C, respectively, representing an increase of 1.24 °C between the two periods.

On average, wind speed during the DP of 2023 was 1.9 m $s^{-1}$, with maximum and minimum values of 2.8 and 0.5 m $s^{-1}$, respectively. In 2024, the mean wind speed was 1.6 m $s^{-1}$, with maximum and minimum values of 3.0 and 1.2 m $s^{-1}$, respectively. Analysis of the results shows that the mean wind speed during the RP was 0.7 m $s^{-1}$.

Net radiation (Rn) values for the irrigated treatment during the DP of 2023 averaged 16.9 MJ $m^{-2}$ per day, with maximum values of 17.2 MJ $m^{-2}$ per day. With the onset of the rainy period, a reduction was observed (12.5 MJ $m^{-2}$ per day), followed by

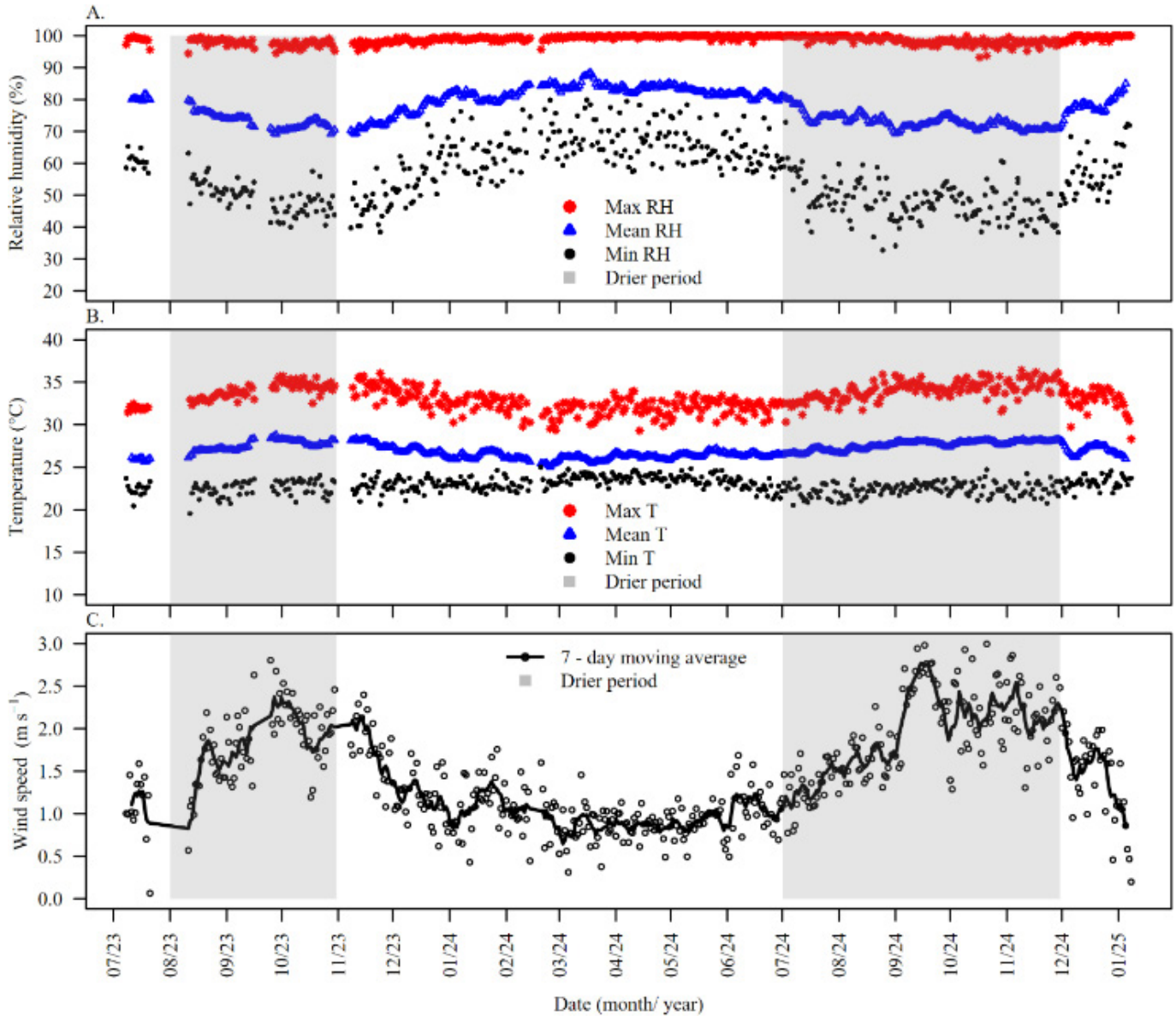


**Figure 3.** Daily maximum, mean, and minimum variation of relative humidity of air - RH (A), air temperature (B), and wind speed (C), distinguishing the dry periods, occurring from August to November 2023 and from July to November 2024

a marked increase with the return of the DP months, reaching values of up to 17.5 MJ $m^{-2}$ per day (Figure 4A). Energy partitioning in the irrigated treatment during the RP of 2023 showed that most of the Rn (12.3 MJ $m^{-2}$ per day) was dissipated as latent heat flux (LE), with a mean value of 7.5 MJ $m^{-2}$ per day, corresponding to approximately 62.7% (Figure 4A).

In contrast, in the treatment where plants were managed under rainfed conditions, mean Rn during the DP of 2023 was 15.5 MJ $m^{-2}$ per day, and energy was predominantly dissipated as sensible heat flux (H), with a value of 8.0 MJ $m^{-2}$ per day, corresponding to 51% (Figure 4B). Similarly under the irrigated treatment, during the RP of 2024, net radiation (12.1 MJ $m^{-2}$ per day) was mainly dissipated as latent heat flux (LE), with a value of 5.65 MJ $m^{-2}$ per day, representing 53.7%.

It is important to note that the study area is located near the Equator; therefore, there are no large seasonal variations in incoming solar radiation throughout the year. Thus, variations in Rn and the radiation balance during rainy and dry periods are mainly influenced by cloud cover, especially during the rainy and dry months (Nyeki et al., 2019; Pinto et al., 2022).

Analysis of the fluxes during the RP of 2024 shows an increase in Rn and differences in the mean microclimate values under irrigated conditions (16.5 MJ $m^{-2}$ per day) (Figure 4A) and rainfed conditions (15.4 MJ $m^{-2}$ per day) (Figure 4B). The increase in Rn during the DP is closely related to a reduction in diffuse radiation due to lower cloudiness. Clear-sky days may result in increased evaporative demand, higher air temperatures, and higher wind speeds due to increased direct radiation, as well as reduced relative humidity (Silva Júnior et al., 2023).

Moreover, in contrast to the DP of 2024, the rainfed treatment during the DP of the same year showed that Rn (15.4 MJ $m^{-2}$ per day) was mainly dissipated through sensible heat flux, accounting for 57.1% (6.1 MJ $m^{-2}$ per day), followed by LE with 42.7% and G with 0.1% (Figure 4B). Agricultural systems in which Rn is predominantly dissipated as sensible heat indicate that energy is being used to heat the air and the plant canopy. The intensification of the sensible heat flux under these conditions may indicate a potential reduction in water-use efficiency, associated with relative water restriction

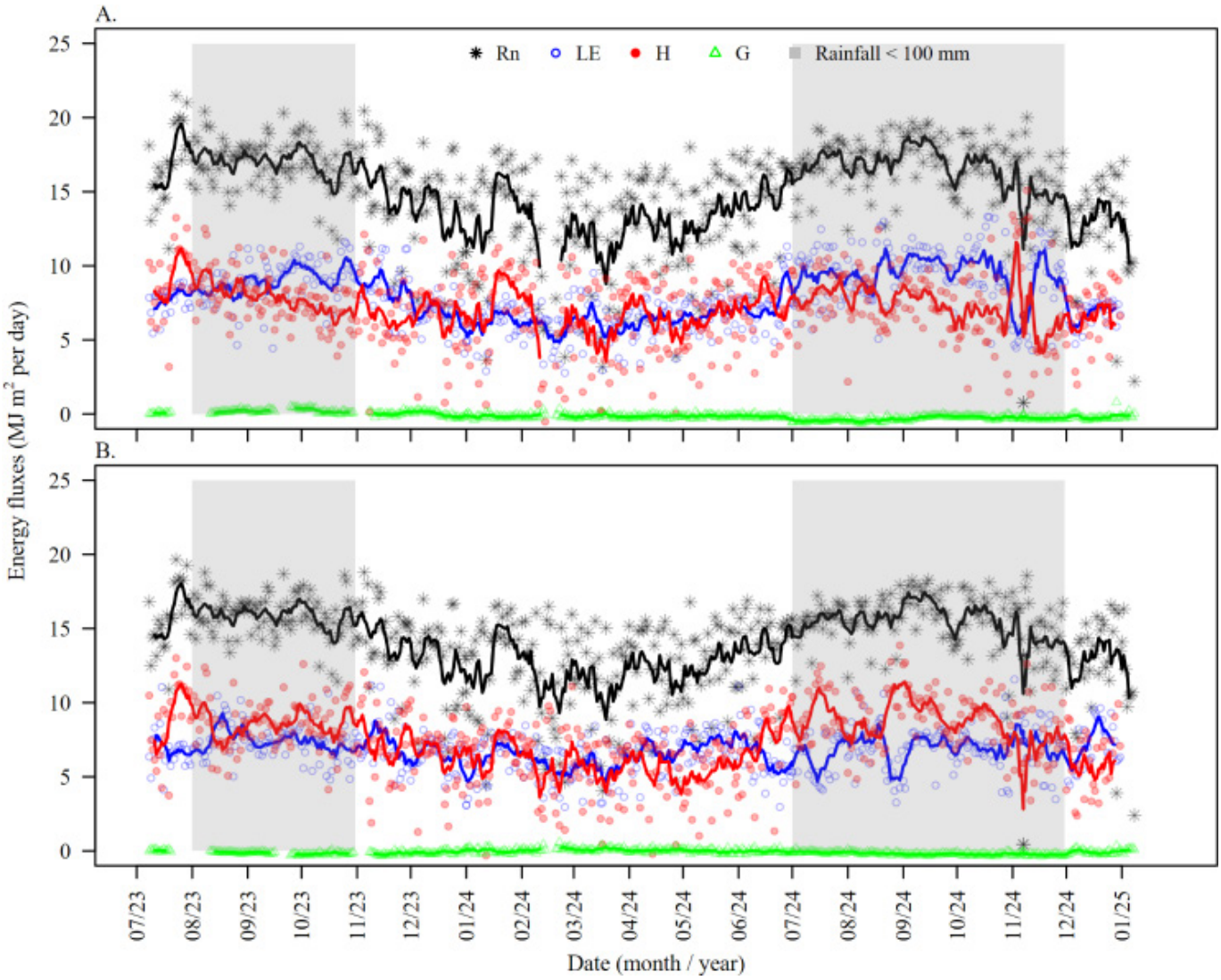


**Figure 4.** Daily variation of net radiation (Rn), latent heat flux (LE), sensible heat flux (H), and soil heat flux (G) of 'Tahiti' acid lime plants under irrigated (A) and rainfed (B) regimes from July 2023 to January 2025, highlighting the dry periods (rainfall < 100 mm per month), occurring from August to November 2023 and from July to November 2024

or physiological responses of the crop to prevailing conditions (Araújo et al., 2022).

On the other hand, still during the DP of 2024, the irrigated treatment showed that although energy dissipation occurred predominantly through latent heat flux (55.9%), there was a marked increase in the proportion of sensible heat flux (44.1%) (Figure 4A). These results differ from those reported by Carvalho et al. (2024), who observed a mean Rn of 13.3 MJ $m^{-2}$ per day and 76.1% dissipation as LE during August, September, October, and November 2021 in a green dwarf coconut plantation irrigated by microsprinklers in Santa Izabel, Pará, Brazil.

One possible explanation is that localized irrigation systems may not be the most suitable for 'Tahiti' acid lime cultivation, considering the spatial arrangement and age of the plants evaluated in this experiment, as well as the soil type (sandy loam texture).

In drip tape irrigation systems, although the applied irrigation depth meets crop water requirements, water is supplied at low application intensity and directly to the root zone. This maintains plants in a physiologically active state but may reduce soil moisture in the upper soil layers, thereby restricting direct evaporation from soil. This characteristic reduces direct evaporation, limiting LE and consequently favoring a relative increase in H, despite continuous water supply (Andrade et al., 2021).

During the DP of 2023, soil moisture in the irrigated system averaged 0.21 ± 0.06 $cm^3$ $cm^{-3}$ at 10 cm, 0.26 ± 0.05 $cm^3$ $cm^{-3}$ at 30 cm, and 0.25 ± 0.06 $cm^3$ $cm^{-3}$ at 50 cm depth (Table 2). In contrast, the rainfed system showed significantly lower values at all depths, with soil moisture of 0.08 ± 0.06 $cm^3$ $cm^{-3}$ at 10 cm, 0.13 ± 0.07 $cm^3$ $cm^{-3}$ at 30 cm, and 0.20 ± 0.04 $cm^3$ $cm^{-3}$ at 50 cm (Table 2).

During the DP of 2024, soil moisture in the irrigated system averaged 0.13 ± 0.07 $cm^3$ $cm^{-3}$ at 10 cm and 0.24 ± 0.05 $cm^3$ $cm^{-3}$ at both 30 and 50 cm depths (Table 2). In contrast, the rainfed system showed significantly lower values at all depths, with soil moisture of 0.09 ± 0.06 $cm^3$ $cm^{-3}$ at 10 and 30 cm and 0.19 ± 0.04 $cm^3$ $cm^{-3}$ at 50 cm (Table 2).

These results reinforce the argument presented above, since the soil moisture at the 10 cm layer is very close to the permanent wilting point of 0.11 $cm^3$ $cm^{-3}$ (Table 1), which may increase soil temperature and, consequently, enhance the sensible heat flux.

It was observed that during the 2024 RP, the albedo ranged from 11.0 to 16.2%, while the sensible heat flux (H) decreased from 8.0 MJ $m^{-2}$ per day to an average of 6.6 MJ $m^{-2}$ per day. During the first three months of the 2024 DP, the albedo decreased from 13.5 to 12.5%, while H increased from 7.0 to 9.0 MJ $m^{-2}$ per day. These results emphasize an inverse relationship between albedo and sensible heat flux (Figure 5).

**Table 2.** Mean soil moisture (± SD) at depths of 10, 30, and 50 cm under irrigated and rainfed systems during rainy and dry periods of 2023–2024

| Period | Soil moisture ($cm^3$ $cm^{-3}$) | | | | | |
|---|---|---|---|---|---|---|
| | Irrigated | | | Rainfed | | |
| | 10 cm | 30 cm | 50 cm | 10 cm | 30 cm | 50 cm |
| Dry period (2023) | 0.21 ± 0.06 a | 0.26 ± 0.05 a | 0.25 ± 0.06 a | 0.08 ± 0.06 b | 0.13 ± 0.07 b | 0.20 ± 0.04 b |
| Rainy period (2024) | 0.23 ± 0.05 a | 0.29 ± 0.01 a | 0.29 ± 0.01 a | 0.21 ± 0.03 b | 0.23 ± 0.02 b | 0.27 ± 0.01 b |
| Dry period (2024) | 0.13 ± 0.07 a | 0.24 ± 0.05 a | 0.24 ± 0.04 a | 0.09 ± 0.06 b | 0.09 ± 0.06 b | 0.19 ± 0.04 b |

Different lowercase letters in the same row and depth indicate significant differences between irrigated and rainfed treatments according to the Wilcoxon rank-sum test ($p < 0.01$)

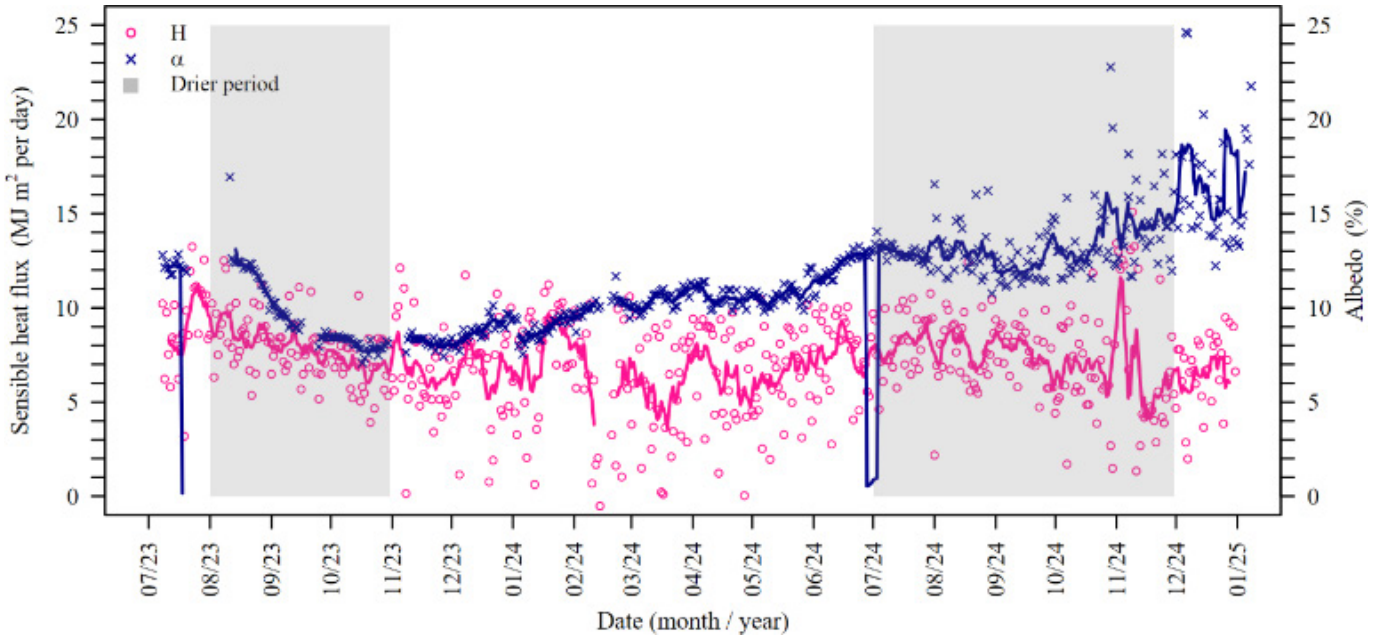


**Figure 5.** Variation in the relationship between sensible heat (H, MJ $m^{-2}$ per day) and albedo (α, %), distinguishing the Dry Periods (DP) occurring from August to November 2023 and from July to November 2024

Additionally, a more pronounced increase in albedo (from 12.5 to 15%) was observed from September 2024 onward, which may have resulted from changes in radiation absorption dynamics, particularly in the infrared band.

The inverse relationship between albedo (α) and sensible heat may be associated with a reduction in leaf density in the inter-row areas (death of spontaneous vegetation) due to water restriction during the DP, leaving the soil excessively exposed (dark coloration). This condition directly affects the reflection of shortwave radiation, especially from July to September. Thus, the lower the albedo, the greater the amount of energy retained within the agricultural system. As a large portion of the area is composed of inter-rows, which remained bare and non-irrigated, most of the net radiation energy was directed to sensible heat in the rainfed treatment.

Recent studies show that changes in vegetation cover and in the spectral response of the surface over time alter albedo, especially in bands correlated with the near-infrared and its interaction with vegetation and soil components, corroborating the hypothesis that seasonal changes in albedo may reflect variations in the absorption dynamics of the terrestrial surface (Li et al., 2023). It is also noteworthy that changes in albedo affect the partitioning of net energy among components, such as sensible heat flux (H) (Sanchez-Mejia et al., 2014).

Figures 6A and B show the temporal variation of ETc and the crop coefficient (Kc) for irrigated and rainfed systems throughout the evaluated period. Due to the high daily variability characteristic of evapotranspiration time series, a 7-day moving average was applied to smooth short-term fluctuations and facilitate the visualization of temporal differences between treatments.

In general, ETc values in the irrigated system were consistently higher than those observed under rainfed conditions, a pattern that becomes more evident when the curves are smoothed with a moving average (Figure 6A). This difference reflects the greater soil water availability in the irrigated system, allowing the crop to maintain higher transpiration rates even during periods of greater atmospheric demand.

The statistical analysis performed using daily values indicated a significant difference between treatments ($p < 0.01$). In 2023, the mean ETc in the irrigated system was 3.7 ± 0.6 mm per day, whereas under rainfed conditions it was 3.0 ± 0.5 mm per day. In 2024, the mean values were 3.7 ± 0.9 mm

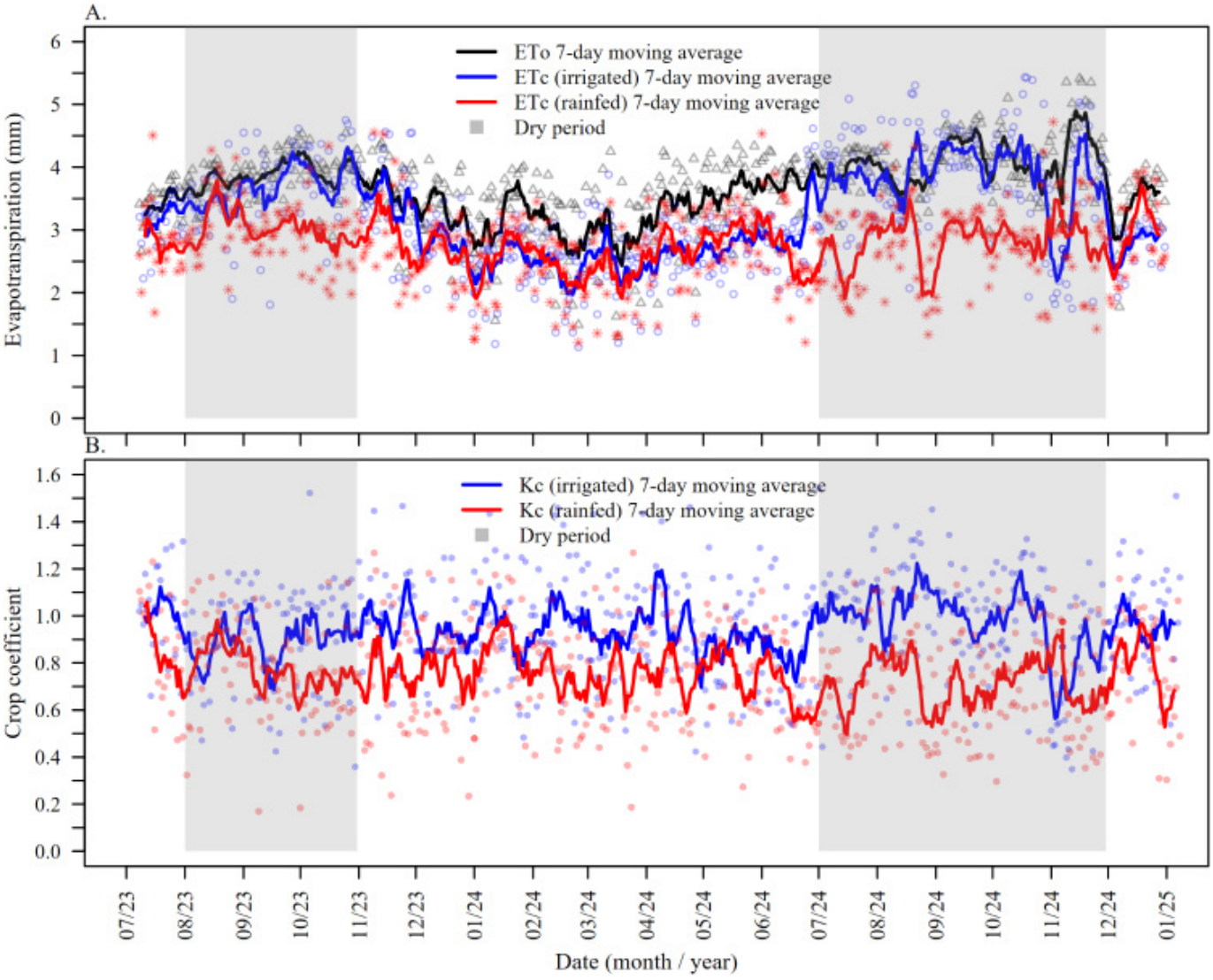


**Figure 6.** Daily variation of reference evapotranspiration (ETo) and crop evapotranspiration under irrigated (ETc, irrigated) and rainfed (ETc, rainfed) conditions (A), and of the crop coefficient—Kc irrigated and Kc rainfed (B), distinguishing the Dry Periods (DP) occurring from August to November 2023 and from July to November 2024

per day for the irrigated system and 2.9 ± 0.6 mm per day for the rainfed system. In percentage terms, the differences were approximately 19 and 22% for 2023 and 2024, respectively (Figure 6A).

The Kc followed the same trend, with statistical differences of approximately 14% in 2023 and 15% in 2024. The mean values were about 1.0 ± 0.2 for irrigated Kc and 0.8 ± 0.2 for rainfed conditions during both periods of lesser precipitation. A study by Pinto et al. (2022) also reported Kc values (0.74 to 0.84) lower than 1 for six-year-old 'Tahiti' acid lime plants. Jamshidi et al. (2020) reported Kc values ranging from 0.67 to 0.97 for sweet orange (*Citrus sinensis*). The low crop coefficient under non-irrigated conditions may be explained by the osmotic adjustment mechanisms of acid lime.

These results indicate that irrigation consistently increased crop evapotranspiration across the evaluated years, highlighting the effect of water availability on maintaining water flux within the soil–plant–atmosphere system.

These results may be related to several factors, including an imbalance in net radiation partitioning in the rainfed microclimate, where energy was predominantly dissipated as sensible heat. This energy imbalance may have led to unfavorable weather conditions, particularly increased air temperature, reduced relative humidity, and, consequently, increased vapor pressure deficit (Silva et al., 2018), resulting in 'Tahiti' acid lime plants exhibiting reduced photosynthetic efficiency.

During the harvest period, when plants were under similar water conditions, the average productivity of irrigated plants was 4.63 t ha$^{-1}$, with a maximum of 7.94 t ha$^{-1}$. In contrast, plants cultivated under rainfed conditions showed an average productivity of 3.71 ± 4.36 t ha$^{-1}$, with a maximum value of 6.75 t ha$^{-1}$ (Figure 7A).

It is worth noting that in the state of Pará, the main harvest period for 'Tahiti' lime occurs between December and April, with peak production concentrated in the first months of the year. In contrast, the off-season extends from July to December, largely coinciding with the DP, resulting in a marked yield reduction in most rainfed orchards (Bárbara et al., 2021).

Figure 7A also shows the temporal variation in yield during the first and second off-season periods. On average, during the first off-season period, productivity under irrigated conditions reached 5.11 ± 3.08 t ha$^{-1}$, whereas plants grown under rainfed conditions produced 2.80 ± 2.20 t ha$^{-1}$, indicating an 82.5% increase promoted by irrigation. During the second off-season period, The superiority of irrigated plants was even more pronounced, with mean productivity values of 9.03 ± 4.88 t ha$^{-1}$ and 1.99 ± 1.13 t ha$^{-1}$ under irrigated and rainfed conditions, respectively, corresponding to a 354% increase.

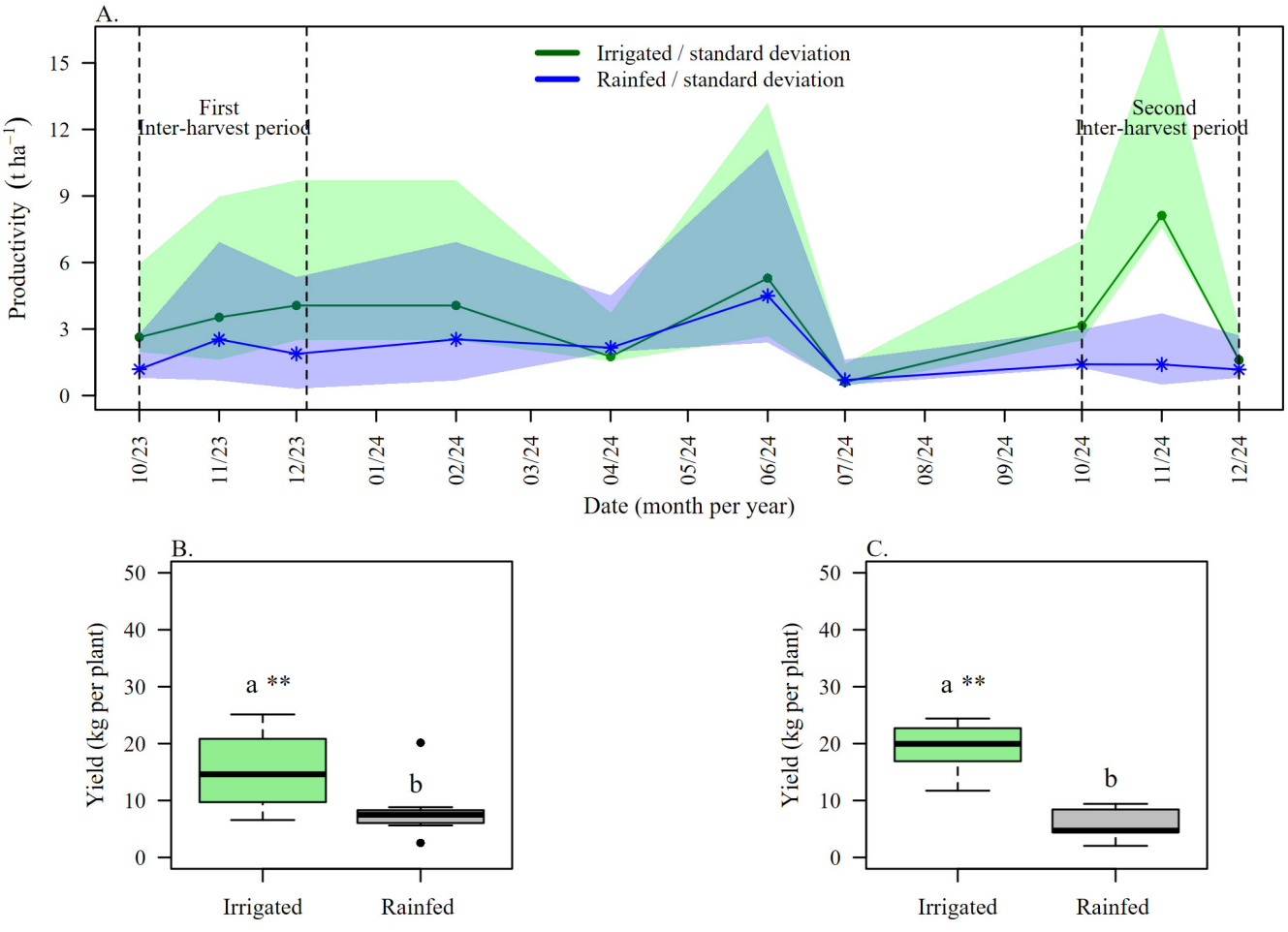


**p < 0.01, significant by the t-test

**Figure 7.** Variation in yield (t ha$^{-1}$) of 'Tahiti' acid lime plants under irrigated and rainfed conditions from October 2023 to December 2024 (A), and statistical analysis of fruit yield (kg per plant) during the first (B) and second (C) inter-harvest periods

The total productivity obtained under irrigation conditions during the 2024 agricultural year was 32.19 t $ha^{-1}$, while under rainfed conditions, it was 14.60 t $ha^{-1}$, representing a 54% reduction. Furthermore, under irrigation, 50.8% of the total annual productivity (16.36 t $ha^{-1}$) was concentrated during the off-season (DP). In contrast, under rainfed conditions, only 24% (3.52 t $ha^{-1}$) of total production occurred during this period. It is also noteworthy that the average productivity in the state of Pará during the 2024 agricultural year was 15.7 t $ha^{-1}$, indicating that irrigation increased productivity by approximately 105%.

These results highlight the importance of irrigation during specific phases of the off-season, as water restriction during the early stages of fruit formation may impair biometric characteristics and reduce fruit number due to premature fruit drop. Conversely, water deficit after fruit set can negatively affect fruit quality attributes (Chen et al., 2022).

During the first off-season, irrigated plants showed statistically higher fruit yield, with a median of approximately 17 kg per plant and a wide positive range, reaching values close to 25 kg per plant. In contrast, rainfed plants exhibited a median yield below 9.5 kg per plant, with very limited variability (Figure 7B). During the second off-season, irrigated plants again showed statistically superior performance, with a median yield of approximately 20 kg per plant and a maximum of approximately 28 kg per plant. In contrast, rainfed plants had a median of 6 kg per plant and lower variability among plants (Figure 7C).

The cumulative fruit production throughout the study period reached 61 kg per plant under irrigated conditions and 29.5 kg per plant under rainfed conditions. Furthermore, considering a planting density of 666.7 plants $ha^{-1}$, the total productivity under irrigation was estimated at approximately 40 t $ha^{-1}$, representing a 42% increase compared to the expected regional production, which was 19.65 t $ha^{-1}$ in 2019 and 28.15 t $ha^{-1}$ in 2020 (IBGE, 2025).

## Conclusions

1. An irrigation depth of 4.42 mm (66.3 L) per plant per day increased the average fruit yield and concentrated 50.8% of the total agricultural production in 2024 during the off-season period.

2. Irrigation maintained crop evapotranspiration (ETc) close to atmospheric demand during the dry periods (DP), with a mean ETc of approximately 3.7 mm per day and a mean Kc of about 1.0 under irrigated conditions. In contrast, the rainfed system showed marked reductions, with a mean ETc of about 2.9 mm per day and a mean Kc of approximately 0.8.

3. Although drip irrigation promoted increased production during the dry periods (DP), radiation balance partitioning showed sensible heat flux values close to latent heat flux, indicating limitations in the surface energy balance and highlighting the need to evaluate alternative irrigation systems, such as microsprinkler or sprinkler irrigation.

**Contribution of authors:** Tayssa M. Franco: Conceptualization, data curation, data analysis, research, methodology, project administration, data presentation, data collection, and data presentation design. Matheus L. Rua: Data analysis, methodology. Miguel G. M. Santos, Paulo A. S. Pardim, Jheny T. de S. Favacho, and Jadson de Jesus R. de Pinho: Data collection. Marcus J. A. de Lima: Data presentation design, text review, and editing. Vandeilson B. Moura: text review and editing. Paulo J. de O. P. de Souza: Project management, supervision, text review, and editing.

**Data Availability Statement:** There are no underlying data associated with the text of the article.

**Conflict of Interest:** No financial or other conflicts of interest were identified during the execution of this study.

**Financing statement:** The research includes the project titled "Agrometeorological technologies as support for the sustainable cultivation of economically important fruit crops in the Amazon." Universal Call for Proposals (Process no. 403902/2021-5), and the project Relationships between vegetative indices, productivity, and evapotranspiration for perennial fruit crops of socioeconomic interest in Eastern Amazonia (Call 08/2022-CNPq/FAPESPA). Productivity grant for the author Paulo J. de O. P. de Souza (Edital nº 09/2022, process 311681/2022-0). Granting a doctoral scholarship to author Tayssa M. Franco (Edital nº. 02/2023, Process 88887.859141/2023-00) by the Brazilian Federal Agency for Support and Evaluation of Graduate Education (CAPES).

## Literature Cited

Allen, R. G. et al. Crop evapotranspiration: guidelines for computing crop water requirements. 1.ed. Rome: FAO, 1998. 300p. Irrigation and Drainage Paper, 56

Alvares, C. A. et al. Köppen climate classification map for Brazil. Meteorologische Zeitschrift, v.22, p.711-728, 2013.

Andrade, S. R. A. et al. Avaliação do desempenho de sistema de irrigação por gotejamento em cultivo de maracujá. Research. Society and Development, v.10, e21710414034, 2021. https://doi.org/10.33448/rsd-v10i4.14034

Araújo, A. B. et al. Sustained deficit irrigation on yield and fruit water quality of dwarf green coconut. Ciência Rural, v.52, e20200674, 2022. https://doi.org/10.1590/0103-8478cr20200674

Bagley, J. E. et al. The influence of land cover on surface energy partitioning and evaporative fraction regimes in the U.S. Southern Great Plains. Journal of Geophysical Research: Atmospheres, v.122, p.5793-5807, 2017. https://doi.org/10.1002/2017JD026740

Bárbara, G. et al. Use of plant regulators in the off-season flower induction of 'Tahiti' acid lime and 'Ponkan' mandarin. American Academic Scientific Research Journal for Engineering. Technology and Sciences, v.84, p.50–59, 2021.

Brandão, V. dos S. et al. Infiltração da água no solo. 3.ed. Viçosa: UFV, 2006.120p.

Carvalho, E. de O. T. de. et al. Net radiation partitioning, evapotranspiration, and crop coefficients of the green dwarf coconut in Santa Izabel do Pará. Brazilian Amazon. Bragantia, v.83, e20230160, 2024. https://doi.org/10.1590/1678-4499.20230160

Chen, F. et al. Effects of water deficit at different growth stages under drip irrigation on fruit quality of citrus in the humid areas of South China. Agricultural Water Management, v.262, 107407, 2022. https://doi.org/10.1016/j.agwat.2021.107407

Diana, E. H. L. et al. O agronegócio e a produtividade do limão Tahiti: Um estudo no município de Marinópolis no Noroeste Paulista. Brazilian Journal of Business, v.3, p.3208-3219, 2021. https://doi.org/10.34140/bjbv3n4-028

IBGE - Instituto Brasileiro de Geografia e Estatística. SIDRA - Sistema IBGE de recuperação automática. 2022. Available on: https://sidra.ibge.gov.br/. Accessed on: Nov. 2025.

Jamshidi, S. et al. Evapotranspiration, crop coefficients, and physiological responses of citrus trees in semi-arid climatic conditions. Agricultural Water Management, v.227, 105838, 2020. https://doi.org/10.1016/j.agwat.2019.105838

Libardi, P. L. Dinâmica da água no solo. 3.ed. São Paulo: EDUSP, 2005. 335p.

Li, X. et al. Responses of land surface albedo to global vegetation greening: An analysis using GLASS data. Atmosphere, v.14, p.2-15, 2023. https://doi.org/10.3390/atmos14010031

Marengo, J. A. et al. The drought of 2010 in the context of historical droughts in the Amazon region. Geophysical Research Letters, v.38, L12703, 2011. https://doi.org/10.1029/2011GL047436

Mualem, Y. A new model for predicting the hydraulic conductivity of unsaturated porous media. Water Resources Research, v.12, p.513-522, 1976. https://doi.org/10.1029/WR012i003p00513

NOAA – National Oceanic and Atmospheric Administration. El Niño and La Niña: related resources. Available on: https://www.cpc.ncep.noaa.gov/products/analysis_monitoring/ensostuff/ONI_v5.php. Accessed on: Jul. 2025.

Nyeki, S. et al. Trends in surface radiation and cloud radiative effect at four Swiss sites for the 1996–2015 period. Atmospheric Chemistry and Physics, v.19, p.13227-13241, 2019. https://doi.org/10.5194/acp-19-13227-2019

Oliveira, A. et al. Gas exchange and growth of bell pepper grown in different substrates under salinity stress. Horticultura Brasileira, v.42, e288866, 2024. https://doi.org/10.1590/s0102-0536-2024-e288866

Pacheco, N. A.; Bastos, T. X. Caracterização climática do município de Capitão Poço – PA. 1ed. Belém: Embrapa Amazônia Oriental, 2001. 17p.

Pinto, J. V. N. et al. Balanço de radiação e partição de fluxos de calor sensível e latente sobre um pomar de lima ácida na Amazônia Oriental. Revista Brasileira de Meteorologia, v.37, p.491-502, 2022. https://doi.org/10.1590/0102-7786374059

Ribeiro, R. M. R. et al. Variabilidade sazonal da Zona de Convergência Intertropical e sua influência sobre o norte da América do Sul. Revista Brasileira de Geografia Física, v.16, p.2798-2810, 2023. https://doi.org/10.26848/rbgf.v16.5.p2798-2810

Sanchez-Mejia, Z. M. et al. Quantifying the influence of deep soil moisture on ecosystem albedo: The role of vegetation. Water Resources Research, v.50, p.4038-4053, 2014. https://doi.org/10.1002/2013WR014150

Schwenck, V. A. X. et al. Coeficiente de cultura por lisímetria da variedade de sorgo forrageiro SF-15 (*Sorghum bicolor* L. Moench). Revista Brasileira de Agricultura Irrigada, v.14, p.3960-3967, 2020. https://doi.org/10.7127/RBAI.V14N101146

Silva, G. S. et al. Aluminum prevents stomatal conductance from responding to vapor pressure deficit in *Citrus limonia*. Environmental and Experimental Botany, v.155, p.662-671, 2018. https://doi.org/10.1016/j.envexpbot.2018.08.017

Silva Júnior, A. C. da. et al. Energy balance, water demand, and crop coefficient of acid lime in the Oriental Amazon. Water, v.15, 1239, 2023. https://doi.org/10.3390/w15061239

Soil Survey Staff. Keys to soil taxonomy. 13.ed. Lincoln: USDA - Natural Resources Conservation Service, 2022. 401p.

Soto, M. A. A.; Kiang, C. H. Avaliação da condutividade hidráulica em dois usos do solo na região central do Brasil. Revista Brasileira de Ciências Ambientais, v.21, p.1-11, 2018. https://doi.org/10.5327/Z2176-947820180169

Souza, E. B. et al. Sazonalidade da precipitação sobre a Amazônia Legal brasileira: clima atual e projeções futuras usando o modelo REGCM4. Revista Brasileira de Climatologia, v.18, p.293-306, 2016. https://doi.org/10.5380/abclima.v18i0.43711

van Genuchten, M. T. A closed-form equation for predicting the hydraulic conductivity of unsaturated soils. Soil Science Society of America Journal, v.44, p.892-898, 1980. https://doi.org/10.2136/sssaj1980.03615995004400050002x